

# Half-Mode Waveguide Based on Gap Waveguide Technology for Rapid Prototyping

Miguel Ferrando-Rocher<sup>1</sup>, Member, IEEE, Jose I. Herranz-Herruzo<sup>1</sup>, Member, IEEE,  
Alejandro Valero-Nogueira<sup>1</sup>, Senior Member, IEEE,  
and Mariano Baquero-Escudero<sup>1</sup>, Senior Member, IEEE

**Abstract**—In this letter, a half-mode waveguide based on gap waveguide (GW) technology for rapid prototyping is explored. Two devices have been designed and measured for demonstration purposes: a power divider and a curved waveguide. Both devices are constructed from two noncontacting metal pieces. Both devices also follow the same design process. In the bottom piece, a horizontally polarized groove GW (GGW) is housed. The height of the groove is about half, which is required to propagate the fundamental mode. The top cover is a uniform pinned surface that acts as a high impedance surface (HIS) over the groove below. Both the power divider and the curved waveguide show measured reflection coefficient values of less than  $-15$  dB in the bandwidth of interest (28–31 GHz) and are in excellent agreement with simulated results. These devices stand out for their ease of fabrication and open a horizon for cheaper and more robust GW designs for mass production.

**Index Terms**—Groove gap waveguide (GGW), half mode waveguide, millimeter-wave devices, rapid prototyping.

## I. INTRODUCTION

THERE is a high demand for Ku- and Ka-band antennas and devices for high throughput satellite systems (HTSs) and the new LEO satellite constellations. In this context, devices with small dimensions and low losses at millimeter-wave frequencies are often required. In search for new solutions that favor greater ease of integration, scalability, and robustness of these devices, the possibility of having narrower waveguides, adjusted to half  $TE_{10}$  mode of the rectangular waveguide, is explored. This new waveguide is completely equivalent to the conventional full waveguide. It consists of simply replacing half waveguide with a high impedance surface (HIS) that behaves like a perfect magnetic conducting plane (PMC). The HIS surface is created with a perfect conductive metal and a set of pins approximately one-quarter of wavelength high. It represents a particular case of gap waveguide (GW) technology [1]–[3]. GW has proven to be an appropriate technique in the millimeter band to assemble all kinds of devices, from filters [4], [5] or transitions [6] to multiband antennas [7], [8].

Manuscript received September 9, 2021; accepted October 2, 2021. This work was supported by the Ministry of Science and Innovation under Project PID2019-107688RB-C22. (Corresponding author: Miguel Ferrando-Rocher.)

The authors are with the Antennas and Propagation Laboratory, Universitat Politècnica de València, 46022 Valencia, Spain (e-mail: miguel.ferrando@ua.es).

Color versions of one or more figures in this letter are available at <https://doi.org/10.1109/LMWC.2021.3119534>.

Digital Object Identifier 10.1109/LMWC.2021.3119534

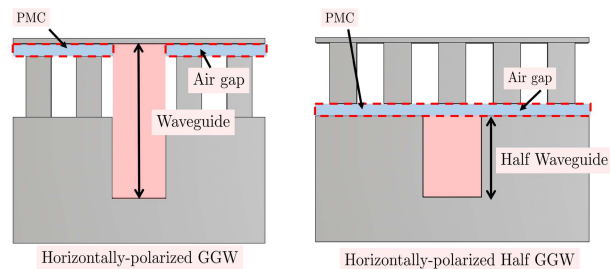


Fig. 1. Different topologies of groove GWs (GGWs). Conventional horizontally polarized GGW (left). Half-mode waveguide based on GW (right).

Typically, in GW, the groove that forms the waveguide is embedded in the bed of nails, all in the same piece, as seen in the left scheme of Fig. 1. Thus, any bends, curves, or transitions in the groove will affect the colliding pins, making them narrower, thinner, or more fragile. Another option is to reconfigure the periodicity of the pins or their width to avoid these manufacturing problems, but these readjustments are not immediate and are only valid for particular solutions. The alternative that we propose in this letter is to machine the waveguide and the HIS created from a bed of nails in separate pieces. The key GW benefit of not requiring metallic contact between pieces is used here. The advantage of this approach is that the machining complexity is simplified with respect to pieces where the feeding networks, cavities, bends, or transitions are housed next to the pins. With this proposal, the manufacture of the pieces is very much relaxed since, on the one hand, it is enough to make the groove on a metal plate, and on the other hand, the HIS part can be standard and reused in other circuits.

Interesting theoretical work was presented in the past addressing this half-mode configuration [9], [10], but, to date, at least to the knowledge of these authors, its actual possibilities in manufactured GW devices have not been studied yet. In this letter, we demonstrate the feasibility of the concept by means of a narrowband one-to-two power divider and a curved waveguide. Sections II–IV present some design criteria, experimental results, and conclusions, respectively.

## II. DESIGN CRITERIA

### A. Waveguide Dispersion With Half-Mode $TE_{10}$

This section details the guidelines for working with a half-mode GGW (HM-GGW). First, the dispersion diagram of an

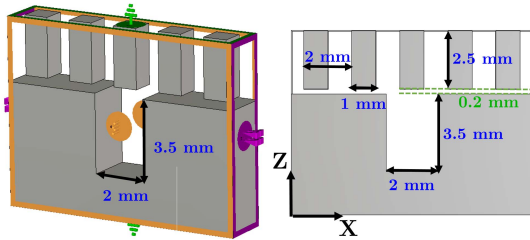


Fig. 2. Cross section of the waveguide and defined boundary conditions to calculate the dispersion diagram. The pink outline indicates air ( $X$ -axis); yellow indicates periodic conditions ( $Y$ -axis); and green indicates an electrical wall ( $Z$ -axis).

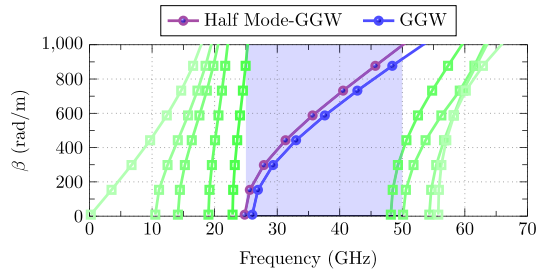


Fig. 3.  $TE_{10}$  half-mode waveguide dispersion diagram using GW technology.

HM-GGW is analyzed. The following data are used for the design of the waveguide: center frequency ( $f_0$ ) of 30 GHz and cutoff frequency ( $f_c$ ) of 22 GHz, which are sufficiently far away from the design frequency band. With these criteria, the pin height is calculated, which should be around  $\lambda/4$  at the operating frequency, i.e., 2.5 mm, although this is a parameter that may be slightly tunable. Extensive studies of the influence of pin height have been addressed in the past [11], [12].

The full waveguide height is calculated from the chosen cutoff frequency, resulting in 7 mm. As seen in Fig. 1, the HM-GGW uses only half of that height, in this case, 3.5 mm. Once the dimensions of the HM-GGW have been obtained, the magnetic wall to be placed on it must be designed. This wall is synthesized using the usual square cross section pins employed in GW technology.

Next, the air gap between the pins and the bottom part containing the half waveguide is defined. It typically ranges from  $\lambda/20$  to  $\lambda/50$ . Larger air gaps are valid and can be used without risk of field leakage as long as they are smaller than  $\lambda/4$ . With these final dimensions (see Fig. 2), the dispersion diagram of the waveguide is obtained. It is shown in Fig. 3. As can be seen, lower and upper modes appear, as well as a typical dispersion curve of the mode of interest along with the working band. Interestingly, that single mode in the band of interest has a dispersion diagram similar and, therefore, similar wide bandwidth to that of the full-height GGW.

### B. One-to-Two Power Divider

A top view schematic of the bottom piece, which has overall dimensions of 50 mm  $\times$  50 mm  $\times$  7 mm, is shown in Fig. 4(a). The input ports are located at the rear, being their dimensions 7.112 mm  $\times$  3.556 mm. A matching step to adapt the input

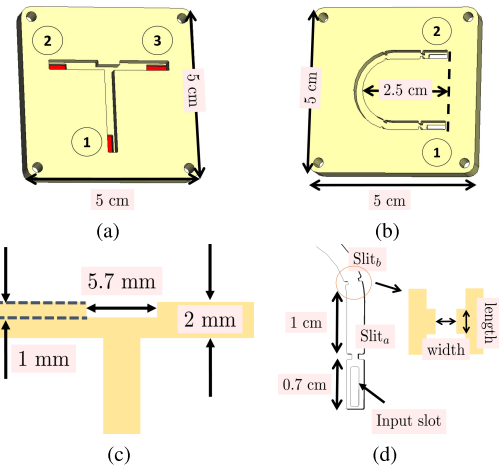


Fig. 4. Schematic and relevant dimensions of the devices. (a) One-to-two power divider. (b) Detail of the dimensions of the power divider slit. (c) Curved waveguide. (d) Detail of the dimensions of the input slits.

slot to the WR-28 has been used. This transition leads to a narrowband performance.

Then, a perfect magnetic wall is used on the top of Fig. 4(a), instead of the pins, to speed up the design and optimization process. Thus, the boundary conditions used are electrical walls in all directions except for the top magnetic wall. Fig. 4(c) shows the dimensions of the optimized divider. With a slit width of 5.7 mm, a length of 1 mm, and a depth identical to the half of a waveguide (3.5 mm), a good input impedance, obtaining a reflection coefficient below  $-15$  dB in a bandwidth greater than 10% (28–31 GHz), is achieved. The next step is to replace that ideal magnetic wall with a real structure, in this case, the GW bed of nails, which will behave as an HIS.

### C. Curved Waveguide

The second device is proposed to demonstrate the feasibility of HM-GGW. Since the pins of the bed of nails are arranged in a square grid in  $X$  and  $Y$ , a straight groove always sees pins aligned with respect to the central axis. Now, a curved waveguide crosses the surface at different angles. This will prove that the relative position of the top lid would not alter the overall performance of the prototypes.

Note that the HIS cover to be used for this prototype is the same as the previous one. A schematic of this waveguide and its relevant dimensions is shown in Fig. 4(b) and (d). Likewise, the conditions for simulating the structure are the same as those described above for the power divider. The dimensions of the input port are 1.3 mm  $\times$  5.9 mm. Finally, the width and length of the capacitive windows (slit<sub>a</sub> and slit<sub>b</sub>) are 0.7 mm  $\times$  1 mm and 1.5 mm  $\times$  0.5 mm, respectively.

## III. EXPERIMENTAL RESULTS

In this section, the simulated and experimental results of both manufactured devices are presented. Fig. 5 shows the simulated  $E$ -field distribution of the HM-GGW in the power divider. Besides, Fig. 6 shows the S-parameters of the transitions used in the power divider and the curved waveguide.

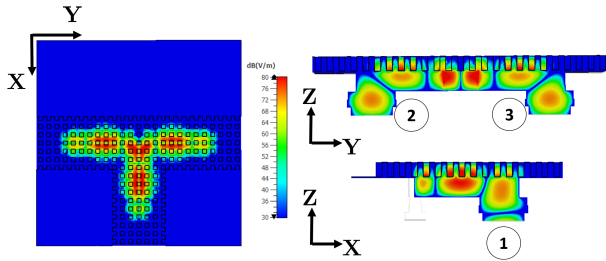
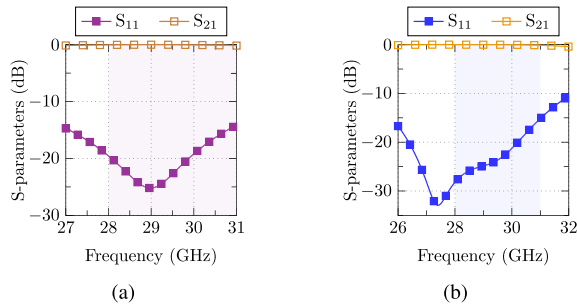
Fig. 5.  $E$ -field distribution of the  $TE_{10}$  HM-GGW.

Fig. 6. Simulated S-parameters of input port transitions. (a) Power divider. (b) Curved waveguide.

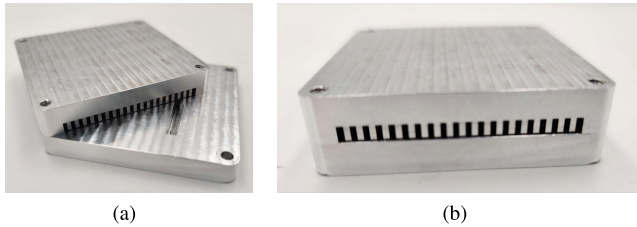
Fig. 7. (a) Curved waveguide assembled with the cover slipped and (b) assembled power divider. The bottom piece of each prototype is shown in Fig. 4; the top piece is a uniform bed of nails. Between the two pieces, there is a  $200\text{-}\mu\text{m}$  air gap.

Fig. 7(a) shows the manufactured curved waveguide, where the bed of nails used as a cover is slipped. The same lid has been used to assemble also the one-to-two power divider [see Fig. 7(b)]. Note that only four screws are used to join both structures.

Fig. 8(a) shows the measured reflection coefficient for the one-to-two power divider, which remains below  $-15$  dB. This threshold obtained is equal to those obtained with the ideal magnetic wall in simulation. Likewise, Fig. 8(c) shows the reflection coefficient for the curved waveguide.

Regarding the power-divider transmission coefficients [see Fig. 8(b)], it is observed that the values range from  $-3.3$  to  $-3.2$  dB. The curved waveguide has an average insertion loss (IL) of  $0.35$  dB [see Fig. 8(d)]. In both devices, the agreement between simulations and measurements is very good for the reflection coefficient, along with  $S_{21}$  and  $S_{31}$  of the power divider. As for the transmission coefficient of the curved waveguide, a slight decay of the IL of  $0.1$  dB is observed compared with the simulation. Either way, the IL is less than  $0.4$  dB in both prototypes, which demonstrates that, despite the air gap between the pieces, the wave is propagated

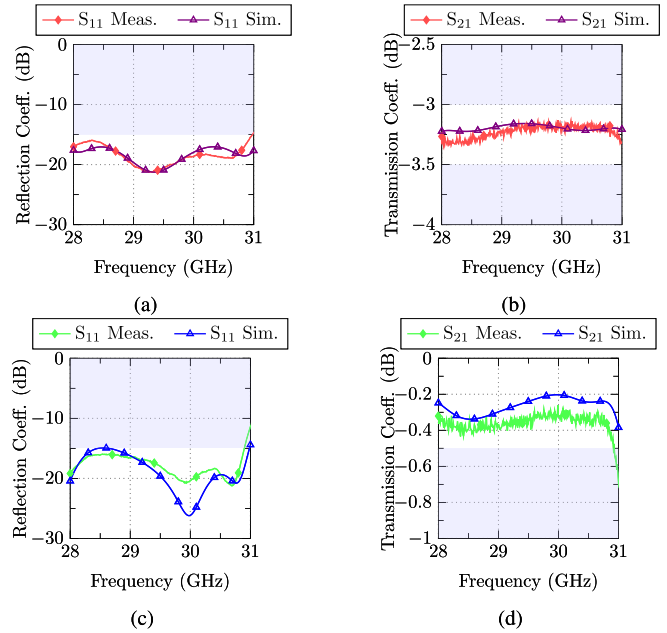


Fig. 8. Measured S-parameters of the one-to-two power divider and of the curved waveguide. (a) and (c) Reflection coefficient. (b) and (d) Transmission coefficient.

TABLE I  
COMPARISON OF GROOVE GAP POWER DIVIDERS  
WITH A BACK FEED PORT

	Band Size	$S_{11} < -10$ dB	$S_{11} < -15$ dB	Mean IL (dB)	Waveguide Type
[13]	V $1 \times 64$	16%	14%	n/a	GGW (Sim.)
[14]	Ka $1 \times 2$	16%	8%	0.22	GGW
[15]	Ka $1 \times 4$	15%	7%	0.25	GGW
This work	Ka $1 \times 2$	13.6%	11.4%	0.25	HM-GGW

through the half-mode waveguide without leakage. Finally, Table I shows a comparison of these results with other state-of-the-art similar works that used conventional GGW instead of this novel HM-GGW.

#### IV. CONCLUSION

A power divider and a curved waveguide employing half-mode  $TE_{10}$  waveguide based on GW have been presented for rapid prototyping in this technology. The devices are constructed from two noncontact metal parts. The bottom piece houses the horizontally polarized GGW. This piece is equivalent to one-half of an  $E$ -plane waveguide. To achieve propagation, the top cover is a uniform surface with pins that act as an HIS over the bottom plate. The measurements of these demonstrators serve to validate the HM-GGW. Besides, the HM-GGW is not restricted to the prototypes here presented, but other devices, such as filters, diplexers, or couplers, are likely feasible with this waveguide. Future lines of research should also study wideband prototypes to confirm their usefulness in a multitude of devices.

## REFERENCES

- [1] P.-S. Kildal, E. Alfonso, A. Valero-Nogueira, and E. Rajo-Iglesias, "Local metamaterial-based waveguides in gaps between parallel metal plates," *IEEE Antennas Wireless Propag. Lett.*, vol. 8, pp. 84–87, 2009.
- [2] P.-S. Kildal, A. U. Zaman, E. Rajo-Iglesias, E. Alfonso, and A. Valero-Nogueira, "Design and experimental verification of ridge gap waveguide in bed of nails for parallel-plate mode suppression," *IET Microw. Antennas Propag.*, vol. 5, no. 3, pp. 262–270, Mar. 2011.
- [3] M. Ferrando-Rocher, A. Valero-Nogueira, J. I. Herranz-Herruzo, A. Berenguier, and B. Bernardo-Clemente, "Groove gap waveguides: A contactless solution for multilayer slotted-waveguide array antenna assembly," in *Proc. 10th Eur. Conf. Antennas Propag. (EuCAP)*, Apr. 2016, pp. 1–4.
- [4] A. Berenguier, V. Fusco, M. Ferrando-Rocher, and V. E. Boria, "A fast analysis method for the groove gap waveguide using transmission line theory," in *Proc. 10th Eur. Conf. Antennas Propag. (EuCAP)*, Apr. 2016, pp. 1–5.
- [5] M. Baquero-Escudero, A. Valero-Nogueira, M. Ferrando-Rocher, B. Bernardo-Clemente, and V. E. Boria-Esbert, "Compact combline filter embedded in a bed of nails," *IEEE Trans. Microw. Theory Techn.*, vol. 67, no. 4, pp. 1461–1471, Apr. 2019.
- [6] M. Ferrando-Rocher, D. Sanchez-Escuderos, J. I. Herranz-Herruzo, and A. Valero-Nogueira, "Design of broadband gap waveguide transitions for millimeter-wave antenna arrays," in *Proc. 48th Eur. Microw. Conf. (EuMC)*, Sep. 2018, pp. 1521–1524.
- [7] M. Ferrando-Rocher, A. Valero-Nogueira, J. I. Herranz-Herruzo, and A. Berenguier, "V-band single-layer slot array fed by ridge gap waveguide," in *Proc. IEEE Int. Symp. Antennas Propag. (APSURSI)*, Jun. 2016, pp. 389–390.
- [8] M. Ferrando-Rocher, J. I. Herranz-Herruzo, A. Valero-Nogueira, and B. Bernardo-Clemente, "Full-metal K-Ka dual-band shared-aperture array antenna fed by combined ridge-groove gap waveguide," *IEEE Antennas Wireless Propag. Lett.*, vol. 18, no. 7, pp. 1463–1467, Jul. 2019.
- [9] E. Tahanian and G. Dadashzadeh, "A novel gap-groove folded-waveguide slow-wave structure for G-band traveling-wave tube," *IEEE Trans. Electron Devices*, vol. 63, no. 7, pp. 2912–2918, Jul. 2016.
- [10] A. Polemi, E. Rajo-Iglesias, and S. Maci, "Analytical dispersion characteristic of a gap-groove waveguide," *Prog. Electromagn. Res. M*, vol. 18, pp. 55–72, 2011.
- [11] E. Rajo-Iglesias, M. Ferrando-Rocher, and A. U. Zaman, "Gap waveguide technology for millimeter-wave antenna systems," *IEEE Commun. Mag.*, vol. 56, no. 7, pp. 14–20, Jul. 2018.
- [12] M. F. Rocher, "Gap waveguide array antennas and corporate-feed networks for mm-wave band applications," Ph.D. dissertation, Dept. Comunicaciones, Universitat Politècnica de València, Valencia, Spain, 2018.
- [13] A. Farahbakhsh, D. Zarifi, A. U. Zaman, and P.-S. Kildal, "Corporate distribution networks for slot array antenna based on groove gap waveguide technology," in *Proc. 10th Eur. Conf. Antennas Propag. (EuCAP)*, Apr. 2016, pp. 1–3.
- [14] A. Tamayo-Domínguez, J. M. Fernández-González, and M. Sierra-Pérez, "Groove gap waveguide in 3-D printed technology for low loss, weight, and cost distribution networks," *IEEE Trans. Microw. Theory Techn.*, vol. 65, no. 11, pp. 4138–4147, Nov. 2017.
- [15] A. Tamayo-Domínguez, J.-M. Fernández-González, and M. Sierra-Pérez, "Metal-coated 3D-printed waveguide devices for mm-wave applications [application notes]," *IEEE Microw. Mag.*, vol. 20, no. 9, pp. 18–31, Sep. 2019.